ACS OMEGA

Open Access

http://pubs.acs.org/journal/acsodf

Article

p-Coumaroylated Lignins Are Natively Produced in Three Rosales Families

Jan Hellinger, John Ralph, and Steven D. Karlen*

Cite This: *ACS Omega* 2025, 10, 6220−6227

Read Online

ACCESS | Metrics & More | Article Recommendations | Supporting Information

ABSTRACT: Carbon-rich plant cell walls contain biopolymers that, with some processing, could replace fossil fuels as a major component of the current petrochemical production. To realize this, biorefineries need to be paired with biomass that during the deconstruction and fractionation processes transforms into the desired products. One component of interest is *p*-coumarate that, in some species, can account for up to 1% of the biomass' dry weight. When *p*-coumarate is present in eudicot cell walls, it is mostly part of the suberin (bark and root), acylates the γ-hydroxy group of the lignin, in part of the tannins, or is a metabolite. The current understanding of eudicot plant cell wall composition is that the lignin is sometimes acylated with acetate and rarely with hydroxycinnamates (*p*-coumarate or ferulate). This study identified a clear division in the Rosales in which three families produce *p*-coumaroylated lignins whereas the other six families showed no evidence of the trait.

INTRODUCTION

With the continual increase in atmospheric greenhouse gases and the destructive impact of global climate change, it has become evident that alternative renewable feedstocks are needed to produce a large portfolio of petrochemicals and fuels that are currently derived from fossil fuels. One such feedstock is lignocellulosic biomass that could become a fossil fuel if incubated in the ground for millions of years.

In a lignocellulosic biorefinery, the plant cell walls are converted to a hydrolysate (predominantly as monomeric sugars with some oligosaccharides) that are then microbially transformed into biofuels and commodity chemicals. The first step in hydrolysate production is the separation of polysaccharides (cellulose and hemicellulose) from the lignin with a fractionation aid: strong acid, base, organic solvents, deep eutectic solvents, homogeneous or heterogeneous catalysts, or enzymatic digestion.[1,2] This deconstruction process often generates undesired microbial toxins from phenolic components of the cell wall polymers, i.e., from lignin, tannins, suberin and, for commelinid monocots, the arabinoxylan bound hydroxycinnamates.[3−7] Understanding the chemical composition of lignin is therefore crucial for optimizing biomass fractionation steps for the microbial production of plant-derived fuels and chemicals.

Lignin makes up 10−25% of the plant cell walls. It is a copolymer formed primarily through the combinatorial radical coupling of monolignols (ML; *p*-coumaryl, coniferyl, and sinapyl alcohols) with the resulting aromatic subunits abbreviated as 4-hydroxyphenyl (H), guaiacyl (G), and syringyl (S).[8] Some clades of plants acylate the γ-hydroxy group of a portion of the MLs via dedicated monolignol acyltransferase enzymes; we will refer to these acylated monolignols as monolignol conjugates (ML-conj).[9] To date, three classes of monolignol acyltransferases have been identified and confirmed with in planta studies: *p*-coumaroyl-CoA monolignol transferase (PMT),[10−14] feruloyl-CoA monolignol transferase (FMT),[15,16] and *p*-hydroxybenzoyl-CoA monolignol transferase (*p*HBMT).[17,18] The ML-conjs are formed in the cytosol and exported to the apoplast where they are oxidized by laccases and/or peroxidases and radical-couple with the growing lignin polymer.[19,20] The ML-conjs couple to the growing lignin polymer chain primarily through the ML moiety of the conjugate. This is because the more electron-deficient phenolate ester (hydroxycinnamate or hydroxy-benzoate) functions as a radical sensitizer for the more electron-rich monolignol, whereby phenolate ester radicals undergo radical transfer to MLs over radical coupling.[21] During active plant deposition of lignin (secondary cell wall formation), the flux of new MLs into the polymerization region outpaces the temporally limited radical generation, so this radical-transfer mechanism dominates. As a result, the three most abundant phenolate esters—*p*-hydroxy-benzoate (*p*HB), *p*-coumarate (*p*CA), and ferulate (FA)—remain largely as free-phenolic pendent groups.[22] As the tissue matures (e.g., in heartwood or as a wound response), the flux of new phenolics decreases,

Received: December 19, 2024
Revised: January 16, 2025
Accepted: January 27, 2025
Published: February 4, 2025

allowing for a fraction of the phenolate esters to radical-couple to other phenolic radicals.

More plant species are being identified as producing phenolic pendent groups, the most abundant of which are *p*CA, found in commelinid monocots that include the grasses (*Poaceae*), *p*HB, that has long been known to be part of Salicaceae lignins (poplars and willows), and acetate, which is on the lignin of many plant species.[23−27] More recently the types of phenolic pendent groups and species that produce them have expanded to include: *p*CA in the eudicot genus Morus[28] and the distantly related Jute (*Corchorus capsularis*)[29,30] and Kenaf (*Hibiscus cannabinus*)[14] of the eudicot family Malvaceae, FA in many clades distributed across the angiosperms,[15] *p*HB in some seagrasses and palms,[31−33] and benzoate (BA) itself at low levels in some palms.[34]

Regardless of how plant biomass is being processed (strong acid, base, organic solvents, deep eutectic solvents, hetero-geneous catalytic systems, or via enzymatic digestion), it is essential to understand the chemical composition of its primary components to maximize their conversion to liquid fuels and commodity chemicals. Depending on the biorefinery structure, the presence of phenolic pendent groups such as *p*CA and FA may lead to toxins inhibiting microbial growth,[35] generate new or increased amounts of coproducts,[36] or alter the severity of conditions required for lignin removal.[16,37] Understanding the diversity of plant species that produce phenolic pendent groups will enable more consensus around design when biorefineries look to use single or mixed feedstocks or when determining a tolerance threshold for toxins present in those feedstocks. Herein, we explore the lignin composition of 15 commercially relevant plant species in 13 different families across six of the nine families of the Rosales order of eudicots.

MATERIALS AND METHODS

General Information. All chemicals used were purchased from Sigma-Aldrich unless otherwise specified.

Plant Material. The sample of *Urtica dioica* was a 4-month-old stem tissue segment growing 2−8″ above the ground. The tissue was harvested by hand from the Wisconsin Energy Institute's mixed prairie demonstration plot. After harvest, the leaves were removed, the stem was washed with water, segmented into 3" pieces, and lyophilized to <5% moisture. The dried stem tissue was stored at room temperature until further processing as described below.

The sample of *Cannabis sativa* was provided to us by Highway 69 Hemp Farms after harvest for CBD production. The tissue used in this study was a segment of mature stem collected from 2−5″ above the ground.

Samples of the other 13 specimens were purchased from Firewood Treasures, MD, as part of a wood identification kit; these samples were sourced from timber that was harvested as commercial lumber.

Extract-Free Cell Wall (CW) Preparations. The dry samples were cut into <1″ pieces and placed into 50 mL stainless steel milling jars with one 25 mm stainless steel ball-bearing. They were then milled to a fine flour on a Retsch MM400 shaker operating at 30 Hz for 3 min. The milled biomass (1 g) was then solvent-extracted with water (3 × 45 mL), 80% ethanol (3 × 45 mL), and acetone (1 × 45 mL). The extracted biomass was then dried under vacuum and stored at room temperature in sealed containers in the dark for the characterization assays.

Enzyme-Lignin (EL) Preparation. A fraction of the dried biomass CW material (750 mg) was ball-milled in 20 mL agate jars with 10 × 10 mm agate ball bearings using a Fritsche Pulverisette 7 planetary ball mill operating at 600 rpm for 35 cycles of 10 min grinding, followed by 5 min rest intervals to avoid excessive heating. The ball-milled samples (650 mg) were suspended in 25.5 mM acetate buffer pH 5.0 (45 mL) and then treated with crude cellulases (Cellulysin, Calbiochem, 20 mg). The samples were then shaken at 250 rpm for 3 days of incubation at 35 °C. After the initial digestion had been completed, the samples were pelletized via a centrifuge (10 min at 1777 rcf on an Eppendorf 5810R). The acetate buffer was then decanted, and the enzymatic digestion was repeated. After two digestion cycles, the samples were washed three times with RO water, the solids suspended in the water, pelleted, and the wash water decanted. Finally, the samples were frozen at −20 °C and lyophilized (pressure <20 mTorr) to produce the enzyme lignin (EL).

Quantification of Phenolic Acids by Alkaline Hydro-ly-sis. Extract-free biomass CW (50 mg) was added to 2 mL screw-top vials (Sarstedt AG & Co., P/N: 72.694.600). *p*-Anisic acid (299.82 μg) was added to the samples as an internal standard, followed by the addition of 2 M sodium hydroxide (1 mL). The samples were then heated to 90 °C for 90 min. After the base hydrolysis, the samples were acidified with 72% sulfuric acid (100 μL) and then placed on ice for at least 5 min to cool the solution. The samples were centrifuged at 14,000 rcf for 1 min in an Eppendorf miniSpin Plus to pellet the suspended solids. The supernatant was removed and filtered through a 0.2 μm nylon filter into 1.5 mL LC-vials. The samples were then placed into a batch queue for LC analysis on a Shimadzu Nexera X2 as described in the Supplemental Data.

2D HSQC (^{1}H−^{13}C) NMR Spectroscopy of Isolated ELs. NMR experiments were performed on enzymatically isolated lignins as previously described.[38,39] The EL (10−20 mg) was dissolved in 500 μL of DMSO-d_6/pyridine-d_5 (4:1, v/v), using sonication and occasional vortexing to dissolve all of the solids. The samples were analyzed using a Bruker Biospin (Billerica, MA) NEO 700 MHz spectrometer equipped with a 5 mm QCI ^{1}H/^{31}P/^{13}C/^{15}N cryoprobe with inverse geometry (proton coils closest to the sample). The ^{1}H−^{13}C correlation experiment was an adiabatic HSQC experiment (Bruker standard pulse sequence 'hsqcetgpsisp2.2'; phase-sensitive gradient-edited-2D HSQC using adiabatic pulses for inversion and refocusing).[40] HSQC experiments were carried out using the following parameters: acquired from 11.65 to−0.66 ppm in F2 (^{1}H) with 3,448 data points (acquisition time, 200 ms) and 215 to −5 ppm in F1 (^{13}C) with 618 increments (F1 acquisition time, 8 ms) of 24 scans with a 1 s interscan delay; the d_{24} delay was set to 0.89 ms (1/8J, J = 140 Hz). The total acquisition time for a sample was 6 h. Processing used typical matched Gaussian apodization (GB = 0.001, LB = −0.5) in F2 and squared cosine-bell in F1 (without using linear prediction). The spectra were referenced using the central DMSO solvent peak (δ_C 39.5, and δ_H 2.49 ppm). The peak assignments were performed manually based on previously reported correlation peaks.[41,42] Volume-integration of contours in HSQC plots was performed manually using fixed rectangular integration boxes in the TopSpin 4.1.4 software, and no correction factors were used; that is, the data represent volume-integrals only. The aromatic signals are reported on a $^{1}/_{2}$*$\mathbf{S}_{2/6}$ + $\mathbf{G}_2$ = 100% basis and the side chains are reported on

https://doi.org/10.1021/acsomega.4c11429
ACS Omega 2025, 10, 6220−6227

an $\mathbf{A}_\alpha$ + $\mathbf{B}_\alpha$ + $\mathbf{C}_\beta$ = 100% basis, in which **A** = β-ether, **B** = phenylcoumaran, **C** = resinol.

Pyrolysis of EL in the Presence of TMAH. About 100 μg of EL was treated with 20 μL of 25 wt % tetramethylammonium hydroxide (TMAH) in methanol. The sample was loaded into a Frontier Lab pyrolyzer and suspended above the furnace. The pyrolysis chamber was flushed with helium four times (pressurized to 18.6 kPa each time) to purge residual air. The sample was then released from the holder and dropped into the furnace to flash-pyrolyze at 500 °C, directly injecting the pyrolysis mixture onto the top of an RXi-5Sil MS column (Restek, 30 m × 0.25 mm × 0.25 μm) in a Shimadzu GCMS-2010. The GC was operated at a constant linear velocity of 28.1 cm/s and an initial pressure of 18.6 kPa. The injection port was set to 300 °C with a split ratio of 50:1. The GC temperature program started at 50 °C for 2 min, then the temperature was ramped at 20 °C/min to 100 °C, and the ramp rate was slowed to 4 °C/min to 150 °C, then to 1 °C/min to 170 °C before being increased to 10 °C/min to 305 °C and held at 305 °C for 24.5 min to clean the column. The total gradient program time was 75 min. The mass-spectrometric (MS) interface was set to 300 °C and the ion-source temperature was set at 280 °C. After a 2.7 min solvent cutoff time, the MS acquired mass spectra from 3−75 min, scanning from 40 to 800 m/z with an event time of 0.3 s. Compound identification was performed by extracting target-ion chromatograms, and the relative intensities of three reference ions were used to validate each compound identity, Table S1. The relative ion ratios were determined from the MS spectra present in the NIST 2011 GC−MS library and previous lignin pyrolysis literature.[43−45] The relative abundances of the compounds in the chromatogram reported in Table 2 represent the relative peak area of the target ion vs the summation area of all quantified target ions in each sample.

Derivatization Followed by Reductive Cleavage (DFRC). The incorporation of monolignol conjugates (ML-*p*CA and ML-FA) into the lignin was determined using the ether-cleaving ester-retaining DFRC method previously established for ML-OH, ML-*p*CA, and ML-FA conjugates.[16,46,47] The DFRC protocol used here is as follows: The lignified cell-wall preparations (10−15 mg of EL or 50 mg of CW, in duplicate) were stirred in 2-dram vials fitted with polytetrafluoroethylene (PTFE) pressure-release caps in acetyl bromide/acetic acid (1/4 v/v, 3 mL). After being heated for 2.5 h at 50 °C, the solvents were removed on a SpeedVac (Thermo Scientific SPD131DDA, 50 °C, 35 min, 50 Torr/min ramp down to 0.1 Torr). The crude films were suspended in absolute ethanol (0.5 mL), dried on the SpeedVac (50 °C, 15 min, 50 Torr/min ramp down to 0.1 Torr), and then suspended in 1,4-dioxane:acetic acid:water (5/4/1 v/v/v, 5 mL) to which nanopowdered zinc (150 mg) was added. The vials were then sealed and sonicated for 1 h to ensure a suspension of solids. The reaction mixtures were then spiked with a mixture of isotopically labeled internal standards (165.8 μg d_8-H, 618.9 μg d_8-G, 551.8 μg d_8-S, 180.7 μg d_{10}-S-*p*CA, 160.7 μg d_{10}-G-FA, 162.7 μg d_{10}-S-FA, and 169.7 μg d_8-S-*p*BA)[46] and quantitatively transferred with dichloromethane (DCM, 2 × 2 mL) into separatory funnels charged with saturated ammonium chloride (10 mL). The phenolics were extracted with DCM (3 × 10 mL), the combined DCM extracts were dried over anhydrous sodium sulfate and filtered, and the solvents were removed via rotary evaporation (water bath at 40 °C) under reduced pressure. The free hydroxyl groups were then acetylated overnight with acetic anhydride and pyridine (1:1 v/v, 4 mL), after which the solvents were removed on a rotary evaporator (water bath at 50 °C) to yield crude oily films. To remove most of the polysaccharide-derived coproducts, the acetylated mixtures were loaded onto solid-phase-extraction (SPE) cartridges (Supelco Supelclean LC-Si SPE tube, 3 mL, P/N: 505048) with DCM (2 × 2.0 mL) and the purified phenolic products eluted with hexanes:ethyl acetate (4:1 v/v, 12 mL). The solvents were then removed by rotary evaporation (water bath at 40 °C) and transferred to GC vials with DCM for final sample volumes of ∼1 mL. Samples were analyzed on a triple-quadrupole GC−MS/MS (Shimadzu GCMS-TQ8030) operating in multiple-reaction-monitoring (MRM) mode calibrated with a 7-point calibration curve based on concentration ratio vs peak area ratio of synthetic standards vs isotopically labeled standards. The GC program and acquisition parameters are listed in Supporting Information Tables S2 and S3, respectively.

RESULTS AND DISCUSSION

The Rosales encompass many economically important food crops, species that are harvested for lumber, used in landscaping, or deployed as cash crops. We recently reported that mulberry trees (*Morus* spp.) produced lignins with *p*CA pendent groups.[28] Interested in identifying closely related plant species that also produce lignins with *p*CA pendent groups, we collected plant specimens across the Rosales to identify how widely distributed this trait was within this economically important clade of plants, as shown in Figure 1. The most

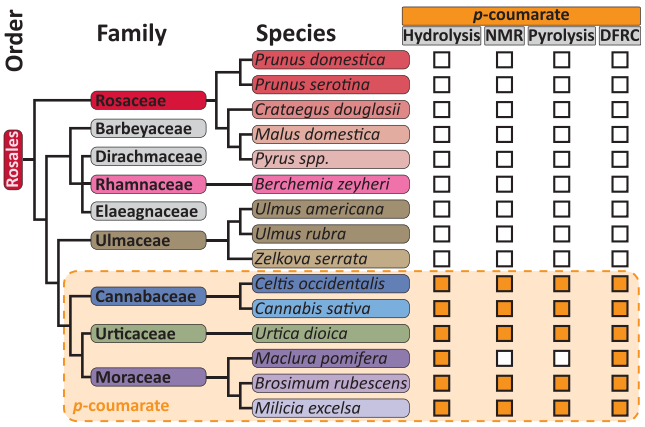

Figure 1. Phylogeny of the species included in this work representing six of the nine families of the Rosales. Chemical assays with positive detection of *p*CA are indicated by a solid orange square; assays with negative detection (less than the threshold of detection) are denoted by empty squares.

distantly related plants studied were found in the Rosaceae, or rose family, and included hawthorn (*Crataegus douglasii*) and common fruit trees such as apple (*Malus domestica*), pear (*Pyrus* spp.), black cherry (*Prunus serotina*), and plum (*Prunus domestica*). Species that are more closely related to the mulberry include some important exotic and common lumber species: pink ivory (*Berchemia zeyheri*, Rhamnaceae), American elm (*Ulmus americana*, Ulmaceae), slippery elm (*Ulmus rubra*, Ulmaceae), zelkova (*Zelkova serrata*, Ulmaceae), hackberry (*Celtis occidentalis*, Cannabaceae), osage orange (*Maclura pomifera*, Moraceae), bloodwood (*Brosimum rubescens*, Moraceae), and iroko (*Milicia excelsa*, Moraceae). We also selected

https://doi.org/10.1021/acsomega.4c11429
ACS Omega 2025, 10, 6220−6227

Table 1. Summary of Characterization Data for the *Rosales* Samples

Characteristic	*Prunus domestica*	*Prunus serotina*	*Crataegus douglasii*	*Malus domestica*	*Pyrus spp.*	*Berchemia zeyheri*	*Ulmus americana*	*Ulmus rubra*	*Zelkova serrata*	*Celtis occidentalis*	*Cannabis sativa*	*Urtica dioica*	*Maclura pomifera*	*Brosimum rubescens*	*Milicia excelsa*
Alkaline saponification															
p-coumaric acid	*n.d.*	*n.d.*	*n.d.*	*n.d.*	*n.d.*	*n.d.*	*n.d.*	*n.d.*	*n.d.*	0.5±0.2	1.0±0.2	29±4	*trace*	1.6±0.5	5.0±1.2
ferulic acid	*n.d.*	*n.d.*	*n.d.*	*n.d.*	*n.d.*	*n.d.*	*n.d.*	*trace*	*n.d.*	*n.d.*	*n.d.*	4.9±0.1	*n.d.*	*n.d.*	*n.d.*
NMR analysis of isolated lignin															
S:G[†]	77:33	80:20	81:19	70:30	68:32	64:36	64:36	25:75	66:34	70:30	59:41	40:60	57:43	27:73	45:55
S/G ratio	3.40	4.07	4.22	2.35	2.16	1.79	1.80	0.34	1.91	2.37	1.43	0.66	1.33	0.37	0.81
p-coumarate	*n.d.*	*n.d.*	*n.d.*	*n.d.*	*n.d.*	*n.d.*	*n.d.*	*n.d.*	*n.d.*	1%	1%	10%	*n.d.*	1%	2%
ferulate	*n.d.*	*n.d.*	*n.d.*	*n.d.*	*n.d.*	*n.d.*	*n.d.*	*n.d.*	*n.d.*	*n.d.*	*n.d.*	*n.d.*	*n.d.*	*n.d.*	*n.d.*
cinnamaldehyde	3%	2%	3%	1%	3%	*n.d.*	5%	7%	7%	5%	21%	7%	5%	5%	4%
benzaldehyde	3%	2%	4%	*n.d.*	3%	*n.d.*	4%	3%	4%	4%	15%	4%	3%	3%	3%
sidechains: β-O-4:β-5:β-β: β-1 (A:B:C:SD)	83:3:8:5	85:3:7:5	84:3:7:5	83:5:9:3	82:5:9:4	82:7:7:3	84:7:4:6	73:18:5:4	84:7:4:6	87:3:5:5	77:7:10:6	74:14:6:5	80:8:8:4	77:17:5:1	80:13:4:3
Lignin composition by DFRC (mg/g EL)															
Monolignols:															
4-hydroxycinnamyl alcohol (H_{OH})	1.1±0.3	0.6±0.1	0.9±0.1	2.8±0.1	1.0±0.1	1.1±0.1	0.5±0.1	1.7±0.1	1.1±0.2	0.1±0.1	0.6±0.1	3.5±0.1	0.7±0.1	0.7±0.1	0.5±0.2
coniferyl alcohol (G_{OH})	65±9	46±1	68±1	56±1	61±1	65±2	65±1	84±2	64±4	87±1	57±2	61±2	85±2	84±3	73±5
sinapyl alcohol (S_{OH})	166±49	210±3	343±2	162±1	203±6	123±3	164±3	45±1	167±15	179±9	125±7	47±1	120±1	51±2	94±10
Monolignol conjugates:															
coniferyl *p*-coumarate (G-*p*CA)	*n.d.*	*n.d.*	*n.d.*	*n.d.*	*n.d.*	*n.d.*	*n.d.*	*n.d.*	*n.d.*	0.1±0.05	0.1±0.05	0.1±0.05	0.1±0.05	0.2±0.05	0.1±0.05
sinapyl *p*-coumarate (S-*p*CA)	*n.d.*	*n.d.*	*n.d.*	*n.d.*	*n.d.*	*n.d.*	*n.d.*	*n.d.*	*n.d.*	*n.d.*	4.4±0.3	10.6±0.4	*n.d.*	*n.d.*	*n.d.*
coniferyl ferulate (G-FA)	*n.d.*	*n.d.*	*n.d.*	*n.d.*	*n.d.*	*n.d.*	*n.d.*	*n.d.*	*n.d.*	*n.d.*	0.2±0.1	2.6±0.1	*n.d.*	*n.d.*	0.9±0.3

[†]½*$S_{2/6}$ + G_2 = 100% monolignol basis

[a]½*S2/6 + G2 = 100% monolignol basis.

hemp (*Cannabis sativa*, Cannabaceae), which is grown for its medicinal oils and high-quality fiber, and stinging nettle (*Urtica dioic*, Urticaceae), a common invasive weed found in many agricultural fields and mixed prairies; nettles are used sometimes to make a tea purported to have health benefits.[48]

Cell-wall-bound phenolics, such as *p*CA, FA, or *p*HB, were reported to be present in many eudicot plants,[49] and some evidence for the possibility that these were lignin-bound was presented.[24] More recently, the gene for forming the ML-*p*CA (monolignol *p*-coumarate) conjugates was identified from kenaf,[14] a distantly related eudicot, augmenting those discovered in grasses.[10−13] *p*CA has been associated with cutin and suberin,[50,51] tannins,[52] and other metabolites.[53−55] For our study, we chose to use a combination of analytical techniques with varying degrees of sensitivity to provide evidence that at least a portion of the *p*CA is bound to the cell wall as a pendent group.

Mild alkaline hydrolysis of extract-free biomass was first used to identify the presence of *p*CA. As hydrolysis cleaves the ester linkage, the detected free *p*CA does not retain any information relating to the chemical origin of the compound, i.e., its regiochemical attachment. Positive hits for *p*CA were found in three families in the Rosales: Moraceae, Urticaceae, and Cannabaceae (Table 1 and Figure 1). These three families cluster closely together as indicated by phylogenetic analysis of the species.[56] Of the positive hits, the largest concentration detected was in *Urtica dioica* at 29.1 mg/100 g of extractive-free cell wall (CW) material, followed by *Milicia excelsa* at 5 mg/100 g. *Brosimum rubescens*, *Celtis occidentalis*, and *Cannabis sativa* contained 1.6 mg, 0.5 mg, and 1 mg/100 g CW material, respectively. Although we detected trace levels of *p*CA in *Maclura pomifera*, the level was below the threshold of quantification for our assay. We also screened for the presence of ferulic acid, which was found to be present at detectable levels in our assay in *Urtica dioica* and *Ulmus rubra*, Table 1.

Lignin fractions were next enzymatically isolated from the cell walls and analyzed by 2D HSQC NMR. This provides chemical characterization data for the lignin polymer and gives some insight into the relative abundance of the lignin subunits.[57] The HSQC spectra showed strong agreement with the saponification data (Figures 1 and 2, and Table 1). *Urtica dioica* again contained the highest level of *p*CA among all of the samples at around 10% calculated based on volume-integration of the $pCA_{2/6}$ peak on a $^1/_2S_{2/6} + G_2 = 100\%$ basis). In agreement with the saponification trends, *Milicia excelsa* contained the second highest concentration of *p*CA at 2%, whereas *Brosimum rubescens*, *Celtis. occidentalis*, and *Cannabis sativa* contained 1% *p*CA. The only discrepancy between the two techniques was for *Maclura pomifera*, in which *p*CA was detected at trace levels by saponification but was apparently below the threshold for detection for HSQC NMR. Also, contrary to the saponification results, there was not an identifiable signal for FA in *Urtica dioica* or *Ulmus rubra*.

As a quick screening technique, we assayed the isolated lignins by pyrolysis−GC−MS in the presence of TMAH. Under such conditions, esters efficiently transesterify to their methyl counterparts, and phenolic hydroxy groups present in the sample or formed by pyrolytic cleavage of the lignin polymer are also methylated.[44] Samples that contained *p*CA pendent groups were identified by the release of methyl 4-methoxycinnamate (Figure S2 and Table 2). The screening assay required the processing of extracted ion chromatograms to identify the presence of the target ion and the use of selected fragment ions to confirm the identity; without this processing, it was difficult to deconvolute some of the target product peaks from coeluting compounds. Under this analysis,

https://doi.org/10.1021/acsomega.4c11429
ACS Omega 2025, 10, 6220−6227

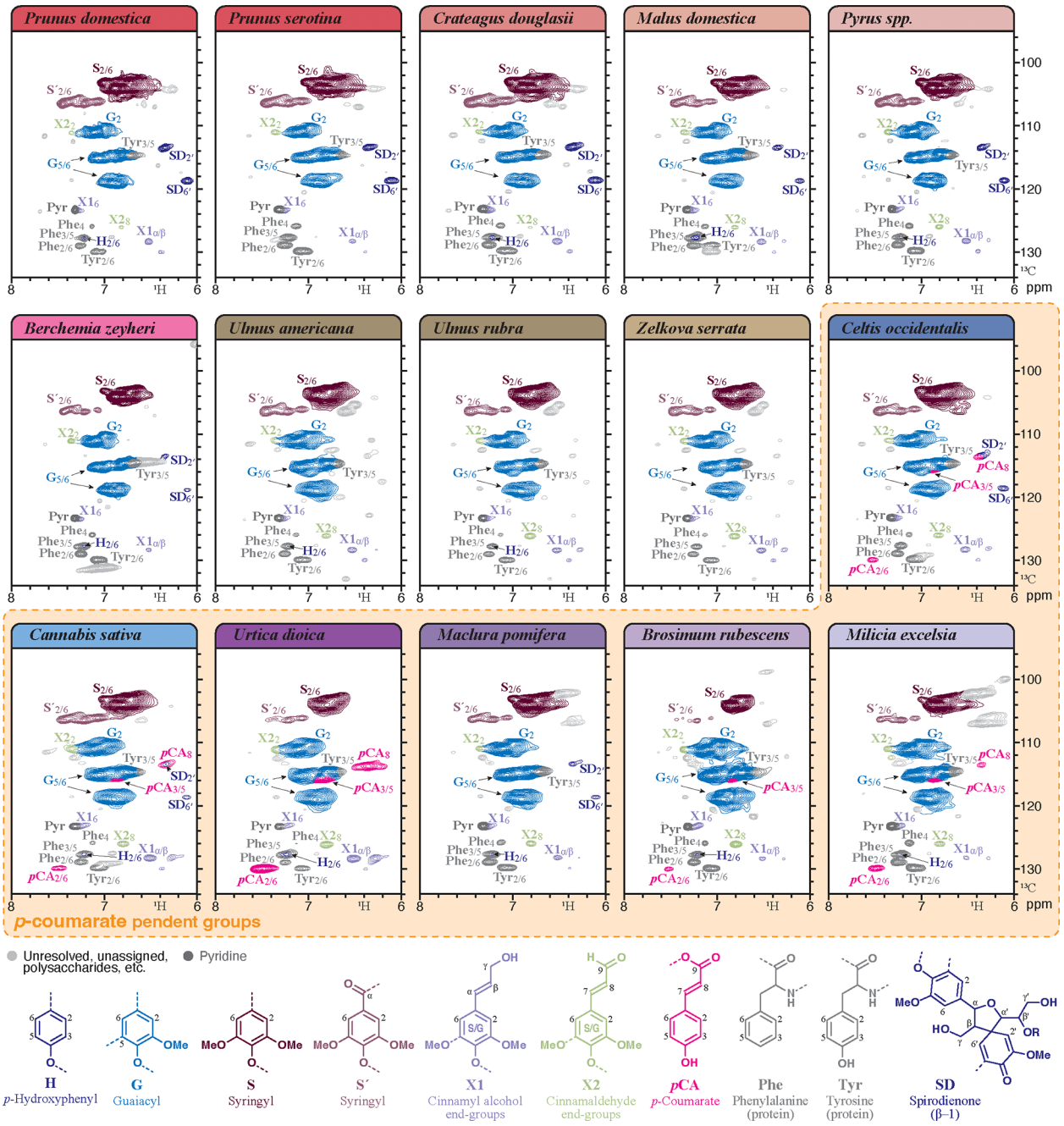

Figure 2. 2D $^{1}H-^{13}C$ HSQC NMR spectra in DMSO-d_6/pyridine-d_5 (4:1, v/v), showing the aromatic regions of enzyme lignins (EL) isolated from representative species of the Rosales. Lignin aromatic subunit structures are shown below the spectra. The substructure units and labels are color-coded to match the correlation peaks assigned in the spectra.

methyl 4-methoxycinnamate could be observed in *Celtis. occidentalis*, *Cannabis sativa*, *Urtica dioica*, *Brosimum rubescens*, and *Milicia excelsa*.

The DFRC assay provides chemical evidence that monolignol conjugates (e.g., ML-*p*CA and ML-FA) have been incorporated, during lignification, into the lignin polymer. DFRC cleaves *β-O*-4 bonds and releases intact ester-linked ML-conjugates; the double bond on the cinnamyl moiety arises only when a *β*-ether is cleaved.[47] Utilizing this property of the assay, the DFRC results from extract-free biomass CWs confirmed the release of ML-*p*CA from *Celtis occidentalis*, *Cannabis sativa*, *Urtica dioica*, *Maclura pomifera*, *Brosimum rubescens*, and *Milicia excelsa*. Detectable levels of coniferyl ferulate esters (G-FA) were also noted from *Cannabis sativa*, *Urtica dioica*, and *Milicia excelsa*. These results support the HSQC NMR, saponification, and pyrolysis data regarding the presence or absence of *p*CA and indicate that, although resource intensive, DFRC is perhaps one of the most sensitive methods for the identification of monolignol conjugates. The results were consistent with the abundance trends from both NMR and saponification with *Urtica dioica* releasing the most ML-*p*CA predominantly as S-*p*CA at 10.6 mg/100 g CW and ML-FA as G-FA at 4.6 mg/100 g CW, followed by *Cannabis sativa* with S-*p*CA at 4.4 mg/100 g CW and G-FA at 0.2 mg/100 g CW. *Milicia excelsa* released more G-FA (0.9 mg/100 g) than G-*p*CA (0.1 mg/100 g) and no detectable S-*p*CA. *Celtis*

https://doi.org/10.1021/acsomega.4c11429
ACS Omega 2025, 10, 6220−6227

Table 2. Identified Products from the GC−MS Pyrograms (Supplemental Figure S2) of ELs[a]

#	Compound	R.T. (min)	Formula	MW	Source	*Prunus domestica*	*Prunus serotina*	*Crateagus douglasii*	*Malus domestica*	*Pyrus spp.*	*Berchemia zeyheri*	*Ulmus americana*	*Ulmus rubra*	*Zelkova serrata*	*Celtis occidentalis*	*Cannabis sativa*	*Urtica dioica*	*Maclura pomifera*	*Brosimum rubescens*	*Milicia excelsa*
1	4-methylanisole	6.91	$C_8H_{10}O$	122.2	H	1.30	1.90	1.54	3.16	1.40	7.94	1.57	2.22	1.01	1.96	2.42	2.78	2.16	2.40	2.07
2	guaiacol	8.11	$C_7H_8O_2$	124.1	G	2.80	2.60	3.65	5.44	2.64	5.70	4.39	7.31	5.41	3.68	4.48	3.03	8.73	8.22	5.94
3	4-methylguaiacol	9.10	$C_8H_{10}O_2$	138.2	G	1.68	1.60	1.51	1.96	1.75	2.18	2.21	3.06	2.14	1.90	2.59	2.10	2.50	3.69	2.49
4	5-methylguaiacol	9.89	$C_8H_{10}O_2$	138.2	G	3.25	3.18	2.86	2.57	2.79	1.72	3.30	2.50	2.26	2.89	2.69	1.36	2.80	2.38	2.00
5	4-methylguaiacol	10.2	$C_8H_{10}O_2$	138.2	G	1.49	1.69	2.31	3.43	1.67	3.71	2.97	5.96	4.48	2.25	3.37	2.24	4.95	7.49	4.78
6	4-ethylguaiacol	12.2	$C_9H_{12}O_2$	152.2	G	2.06	2.27	2.22	2.49	2.05	2.03	2.75	3.78	2.59	2.22	2.82	1.53	3.25	4.13	2.55
7	4-methylsyringol	13.0	$C_9H_{12}O_3$	168.2	S	3.25	3.08	3.14	2.49	2.76	3.16	2.63	1.20	3.35	2.46	2.31	1.19	2.21	1.35	1.70
8	syringol	14.1	$C_8H_{10}O_3$	154.2	S	7.37	7.55	11.8	9.49	6.18	7.72	7.57	3.84	10.1	6.89	5.09	1.36	10.3	4.22	4.51
9	1,2,4-trimethoxybenzene	14.6	$C_9H_{12}O_3$	168.2	G	0.94	0.72	0.47	0.56	0.84	0.61	0.66	0.75	0.51	0.67	0.80	0.78	0.56	0.74	0.81
10	1,2,3-trimethoxy-5-methylbenzene	15.4	$C_{10}H_{14}O_3$	182.2	S	6.75	7.38	7.80	6.73	6.29	5.00	6.30	3.41	6.23	6.12	5.85	2.80	5.65	3.99	4.69
11	*cis*-4-propenylveratrole	16.7	$C_{11}H_{14}O_2$	178.2	G	0.56	0.49	0.20	0.27	0.54	0.00	0.74	0.88	0.19	0.67	0.63	0.61	0.31	0.49	0.37
12	4-methylsyringol	16.7	$C_9H_{12}O_3$	168.2	S	4.90	5.53	7.94	6.66	4.70	5.18	5.55	3.49	7.99	4.68	4.71	1.24	6.21	4.15	3.95
13	3,4-dimethoxybenzaldehyde	17.9	$C_9H_{10}O_3$	166.2	G	5.86	4.99	4.48	6.54	5.82	5.10	7.59	12.3	6.24	7.80	8.62	7.01	7.17	10.7	9.84
14	*trans*-4-propenylveratrole	18.2	$C_{11}H_{14}O_2$	178.2	G	3.45	2.86	2.25	2.60	3.47	2.33	4.11	5.23	2.65	3.83	4.03	3.46	3.11	4.06	3.22
15	1,2,3-trimethoxy-5-(2-propenyl)benzene	19.9	$C_{12}H_{16}O_3$	208.2		1.06	1.15	1.21	0.91	0.91	0.70	1.16	0.49	1.07	0.92	0.96	0.40	0.74	0.47	0.54
16	1-(3,4-dimethoxyphenyl)ethanone	20.7	$C_{10}H_{12}O_3$	180.2	G	*n.d.*	*n.d.*	*n.d.*	*n.d.*	*n.d.*	*n.d.*	*n.d.*	9.51	*n.d.*	*n.d.*	*n.d.*	4.85	*n.d.*	8.77	*n.d.*
17	methyl 3,4-dimethoxybenzoate	21.6	$C_{10}H_{12}O_4$	196.2	G	6.74	5.81	4.39	7.61	7.32	6.21	7.94	9.99	5.39	7.60	7.04	7.63	7.03	8.43	9.76
18	3,4,5-trimethoxybenzaldehyde	22.0	$C_{10}H_{12}O_4$	196.2		15.2	13.4	14.5	11.6	11.6	8.14	11.0	5.29	10.1	10.8	10.1	5.24	9.02	4.77	7.24
19	*cis*-2,6-dimethoxy-4-propenylphenol	23.0	$C_{11}H_{14}O_3$	194.2	S	2.53	2.35	1.17	1.78	2.61	1.38	3.28	4.19	1.15	3.30	3.01	2.92	1.84	2.64	2.79
20	*trans*-2,6-dimethoxy-4-propenylphenol	23.6	$C_{11}H_{14}O_3$	194.2	S	2.55	2.33	1.05	1.57	2.69	1.12	3.19	4.11	0.95	3.30	2.86	2.91	1.68	2.43	2.42
21	1,2,3-trimethoxy-5-(2-propenyl)benzene	23.9	$C_{12}H_{16}O_3$	208.3		5.12	8.09	6.71	4.83	7.13	4.41	6.74	2.57	5.54	6.77	5.59	2.51	3.84	2.22	3.25
22	**methyl 4-methoxycinnamate**	**25.6**	**$C_{11}H_{12}O_3$**	**192.2**	***p*CA**	***n.d.***	***n.d.***	***n.d.***	***n.d.***	***n.d.***	***n.d.***	***n.d.***	***n.d.***	***n.d.***	**4.81**	**5.29**	**25.2**	***n.d.***	**2.81**	**6.61**
23	methyl 3,4,5-trimethoxybenzoate	27.3	$C_{11}H_{14}O_5$	226.2	S	15.6	11.7	10.2	7.92	14.2	6.93	9.96	3.95	6.81	9.40	7.84	5.50	6.18	3.53	6.55
24	methyl palmitate	39.2	$C_{17}H_{34}O_2$	270.5		5.54	9.31	8.57	9.42	10.6	18.7	4.44	4.02	13.9	5.15	6.91	11.4	9.77	5.97	12.0

[a]Samples pyrolyzed at 500 °C in the presence of tetramethylammonium hydroxide (TMAH). Values are relative percentage of the identified compounds base peak areas, *n.d.* = not detected.

[a]Samples pyrolyzed at 500 °C in the presence of tetramethylammonium hydroxide (TMAH). Values are relative percentage of the identified compounds base peak areas, *n.d.* = not detected.

occidentalis, *Maclura pomifera*, and *Brosimum rubescens* all released only G-*p*CA detectable at levels of ∼0.1 mg/100 g CW. S-FA was not detected from any samples despite being present in a variety of commelinid monocots.[15]

CONCLUSIONS

Now that the previously accepted notion that only commelinid monocots have lignin-bound *p*CA has been overturned, the list of eudicots confirmed to produce and incorporate ML-*p*CA into their lignins continues to expand. Currently, the species are all in the Rosids, with one species (kenaf) from the Malvids clade, and this current work reports many species within the Rosales order of the Fabids. These eudicot species consist of trees grown for commercial lumber, some crops grown for use in textiles and for their chemical extractives, and a common weed found in many agricultural plots. Although the amount of ML-*p*CA derived from many of these species is modest compared to that from many grasses, the presence of polymers derived in part from the presence of ML-*p*CA in the lignification monomer pool indicates some favorable driving force guiding plants to upregulate their production of the PMT enzymes that are required for making these conjugates or augmenting them with other more efficient PMTs. This also provides us with an array of potential feedstocks from which we could extract and isolate *p*CA without the nearly equivalent level of FA contamination present in grasses, allowing for simpler purification.

ASSOCIATED CONTENT

Data Availability Statement

The data underlying this study are available in the published article and its Supporting Information.

Supporting Information

The Supporting Information is available free of charge at https://pubs.acs.org/doi/10.1021/acsomega.4c11429.

Supplemental tables and figures with Pyrolysis−GC−MS, GC-MRM-MS, and HSQC NMR data (PDF)

AUTHOR INFORMATION

Corresponding Author

Steven D. Karlen − *Department of Energy Great Lakes Bioenergy Research Center, Wisconsin Energy Institute, University of Wisconsin-Madison, Madison, Wisconsin 53726, United States;* orcid.org/0000-0002-2044-8895; Email: skarlen@wisc.edu

Authors

Jan Hellinger − *Department of Energy Great Lakes Bioenergy Research Center, Wisconsin Energy Institute, University of Wisconsin-Madison, Madison, Wisconsin 53726, United States;* orcid.org/0000-0002-4489-6713

John Ralph − *Department of Energy Great Lakes Bioenergy Research Center, Wisconsin Energy Institute, University of Wisconsin-Madison, Madison, Wisconsin 53726, United States; Department of Biochemistry, University of Wisconsin-*

Madison, Madison, Wisconsin 53706, United States;
orcid.org/0000-0002-6093-4521

Complete contact information is available at:
https://pubs.acs.org/10.1021/acsomega.4c11429

Author Contributions

The manuscript was written through the contributions of all authors. Conceptualization: S.K.; methodology: S.K., J.R.; investigation: J.H., S.K.; resources: J.R., S.K.; data curation: J.H., S.K.; writing − original draft: J.H., S.K.; writing − review & editing: J.H., J.R., S.K.; project administration: S.K., J.R.; and funding acquisition: J.R., S.K.

Funding

This work was funded by the DOE Great Lakes Bioenergy Research Center (DOE BER Office of Science DE-SC0018409).

Notes

The authors declare no competing financial interest.

■ ACKNOWLEDGMENTS

The Wisconsin Energy Institute, Highway 69 Hemp Farms, and Firewood Treasures kindly provided us with the samples used in this study.

■ ABBREVIATIONS

GC, gas chromatography; MS, mass spectroscopy; MRM, multiple-reaction-monitoring; NIST, national institute of standards and technology; NMR, nuclear magnetic resonance (spectrometry); HSQC, heteronuclear single-quantum coherence; SD, spirodienone; SPE, solid-phase-extraction; DFRC, derivatization followed by reductive cleavage; CW, extract-free cell walls; EL, enzymatically isolated lignins; DMSO, dimethyl sulfoxide; DCM, dichloromethane; PTFE, polytetrafluoroethylene; TMAH, tetramethylammonium hydroxide; ML, monolignol; BA, benzoate; *p*HB, *p*-hydroxybenzoate; *p*CA, *p*-coumarate; FA, ferulate; H, 4-hydroxyphenyl; G, guaiacyl; S, syringyl; ML-conj, monolignols with acylated γ-hydroxy group are monolignol conjugates; PMT, *p*-coumaroyl-CoA:mono-lignol transferase; FMT, feruloyl-CoA:monolignol transferase; *p*HBMT, *p*-hydroxybenzoyl-CoA:monolignol transferase; RO, Reverse Osmosis

■ REFERENCES

(1) Zhang, B.; Biswal, B. K.; Zhang, J.; Balasubramanian, R. Hydrothermal treatment of biomass feedstocks for sustainable production of chemicals, fuels, and materials: Progress and perspectives. *Chem. Rev.* **2023**, *123*, 7193−7294.
(2) Schutyser, W.; Renders, T.; Van den Bosch, S.; Koelewijn, S.-F.; Beckham, G. T.; Sels, B. F. Chemicals from lignin: an interplay of lignocellulose fractionation, depolymerisation, and upgrading. *Chem. Soc. Rev.* **2018**, *47* (3), 852−908.
(3) Quideau, S.; Ralph, J. Lignin-ferulate cross-links in grasses. Part 4. Incorporation of 5−5-coupled diferulate into lignin. *Journal of the Chemical Society, Perkin Transactions 1* **1997**, No. 16, 2351−2358.
(4) Azuma, J.-I.; Koshijima, T. Lignin−carbohydrate complexes from various sources. *Methods Enzymol.* **1988**, *161*, 12−18.
(5) Ralph, J.; Hatfield, R. D.; Grabber, J. H.; Jung, H. G.; Quideau, S.; Helm, R. F. Cell wall cross-linking in grasses by ferulates and diferulates. In *Lignin and Lignan Biosynthesis*, Lewis, N. G.; Sarkanen, S., Eds.; Amer. Chem. Soc. Symp. Ser.; American Chemical Society: Washington, DC, 1998; Vol. *697*, pp 209−236.
(6) Ralph, J.; Bunzel, M.; Marita, J. M.; Hatfield, R. D.; Lu, F.; Kim, H.; Schatz, P. F.; Grabber, J. H.; Steinhart, H. Peroxidase-dependent cross-linking reactions of *p*-hydroxycinnamates in plant cell walls. *Phytochemistry Reviews* **2004**, *3* (1), 79−96.
(7) Ralph, J. Hydroxycinnamates in lignification. *Phytochemistry Reviews* **2010**, *9* (1), 65−83.
(8) Boerjan, W.; Ralph, J.; Baucher, M. Lignin biosynthesis. *Annual Reviews in Plant Biology* **2003**, *54*, 519−546.
(9) Ralph, J.; Kim, H.; Lu, F.; Smith, R. A.; Karlen, S. D.; Nuoendagula; Yoshioka, K.; Eugene, A.; Liu, S.; Sener, C.; Ando, D.; Chen, M.-J.; Li, Y.; Landucci, L. L.; Ralph, S. A.; Timokhin, V. I.; Lan, W.; Rencoret, J.; del Río, J. C., Lignins and lignification: New developments and emerging concepts. In *Recent Advances in Polyphenol Research*, Quideau, S.; Salminen, J.-P.; Wähälä, K.; de Freitas, V., Eds.; Wiley-Blackwell: Oxford, UK, 2023; Vol. *8*, pp 1−50.
(10) Withers, S.; Lu, F.; Kim, H.; Zhu, Y.; Ralph, J.; Wilkerson, C. G. Identification of a grass-specific enzyme that acylates monolignols with *p*-coumarate. *J. Biol. Chem.* **2012**, *287* (11), 8347−8355.
(11) Hatfield, R. D.; Marita, J. M.; Frost, K.; Grabber, J. H.; Lu, F.; Kim, H.; Ralph, J. Grass lignin acylation: *p*-coumaroyl transferase activity and cell wall characteristics of C3 and C4 grasses. *Planta* **2009**, *229* (6), 1253−1267.
(12) Marita, J. M.; Hatfield, R. D.; Rancour, D. M.; Frost, K. E. Identification and suppression of the *p*-coumaroyl CoA:hydroxycinnamyl alcohol transferase in *Zea mays* L. *Plant Journal* **2014**, *78* (5), 850−864.
(13) Petrik, D. L.; Karlen, S. D.; Cass, C. L.; Padmakshan, D.; Lu, F.; Liu, S.; Le Bris, P.; Antelme, S.; Santoro, N.; Wilkerson, C. G.; Sibout, R.; Lapierre, C.; Ralph, J.; Sedbrook, J. C. *p*-Coumaroyl-CoA:Monolignol Transferase (PMT) acts specifically in the lignin biosynthetic pathway in *Brachypodium distachyon*. *Plant Journal* **2014**, *77* (5), 713−726.
(14) Mottiar, Y.; Smith, R. A.; Karlen, S. D.; Ralph, J.; Mansfield, S. D. Evolution of *p*-coumaroylated lignin in eudicots provides new tools for cell wall engineering. *New Phytologist* **2023**, *237* (1), 251−264.
(15) Karlen, S. D.; Zhang, C.; Peck, M. L.; Smith, R. A.; Padmakshan, D.; Helmich, K. E.; Free, H. C. A.; Lee, S.; Smith, B. G.; Lu, F.; Sedbrook, J. C.; Sibout, R.; Grabber, J. H.; Runge, T. M.; Mysore, K. S.; Harris, P. J.; Bartley, L. E.; Ralph, J. Monolignol ferulate conjugates are naturally incorporated into plant lignins. *Sci. Adv.* **2016**, *2* (10), No. e1600393. 1−9
(16) Wilkerson, C. G.; Mansfield, S. D.; Lu, F.; Withers, S.; Park, J.-Y.; Karlen, S. D.; Gonzales-Vigil, E.; Padmakshan, D.; Unda, F.; Rencoret, J.; Ralph, J. Monolignol ferulate transferase introduces chemically labile linkages into the lignin backbone. *Science* **2014**, *344* (6179), 90−93.
(17) Zhao, Y.; Yu, X.; Lam, P. Y.; Zhang, K.; Tobimatsu, Y.; Liu, C. J. Monolignol acyltransferase for lignin *p*-hydroxybenzoylation in *Populus*. *Nature Plants* **2021**, *7*, 1288−1300.
(18) de Vries, L.; MacKay, H. A.; Smith, R. A.; Mottiar, Y.; Karlen, S. D.; Unda, F.; Muirragui, E.; Bingman, C.; Vander Meulen, K.; Beebe, E. T.; Fox, B. G.; Ralph, J.; Mansfield, S. D. *p*HBMT1, a BAHD-family monolignol acyltransferase, mediates lignin acylation in poplar. *Plant Physiology* **2022**, *188* (2), 1014−1027.
(19) Zhu, Y.; Regner, M.; Lu, F.; Kim, H.; Mohammadi, A.; Pearson, T. J.; Ralph, J. Preparation of monolignol γ-acetate, γ-*p*-hydroxycinnamate, and γ-*p*-hydroxybenzoate conjugates: Selective deacylation of phenolic acetates with hydrazine acetate. *RSC Adv.* **2013**, *3* (44), 21964−21971.
(20) Mottiar, Y.; Vanholme, R.; Boerjan, W.; Ralph, J.; Mansfield, S. D. Designer lignins: Harnessing the plasticity of lignification. *Curr. Opin. Biotechnol.* **2016**, *37* (1), 190−200.
(21) Hatfield, R. D.; Ralph, J.; Grabber, J. H. A potential role of sinapyl *p*-coumarate as a radical transfer mechanism in grass lignin formation. *Planta* **2008**, *228*, 919−928.
(22) Unda, F.; de Vries, L.; Karlen, S. D.; Rainbow, J.; Zhang, C.; Bartley, L. E.; Kim, H.; Ralph, J.; Mansfield, S. D. Enhancing monolignol ferulate conjugate levels in poplar lignin via OsFMT1. *Biotechnol. Bioefuls Bioprod.* **2024**, *17* (1), 97.
(23) Smith, D. C. C. Ester groups in lignin. *Nature* **1955**, *176*, 267−268.

(24) Smith, D. C. C. *p*-Hydroxybenzoate groups in the lignin of aspen (*Populus tremula*). *Journal of the Chemical Society* **1955**, 2347−2351.
(25) Ralph, J. An unusual lignin from Kenaf. *J. Nat. Prod.* **1996**, *59* (4), 341−342.
(26) del Río, J. C.; Marques, G.; Rencoret, J.; Martinez, A. T.; Gutierrez, A. Occurrence of naturally acetylated lignin units. *J. Agric. Food Chem.* **2007**, *55* (14), 5461−5468.
(27) Lu, F.; Ralph, J. Novel tetrahydrofuran structures derived from *β*−*β*-coupling reactions involving sinapyl acetate in Kenaf lignins. *Organic & Biomolecular Chemistry* **2008**, *6* (20), 3681−3694.
(28) Hellinger, J.; Kim, H.; Ralph, J.; Karlen, S. D. *p*-Coumaroylation of lignin occurs outside of Commelinid monocots in the eudicot genus *Morus* (mulberry). *Plant Physiology* **2023**, *191* (2), 854−861.
(29) del Río, J. C.; Rencoret, J.; Marques, G.; Li, J. B.; Gellerstedt, G.; Jimenez-Barbero, J.; Martinez, A. T.; Gutierrez, A. Structural characterization of the lignin from jute (*Corchorus capsularis*) fibers. *J. Agric. Food Chem.* **2009**, *57* (21), 10271−10281.
(30) Shafrin, F.; Ferdous, A. S.; Sarkar, S. K.; Ahmed, R.; Amin, A.; Hossain, K.; Sarker, M.; Rencoret, J.; Gutierrez, A.; Del Rio, J. C.; Sanan-Mishra, N.; Khan, H. Modification of monolignol biosynthetic pathway in jute: Different gene, different consequence. *Sci. Rep.* **2017**, *7*, No. 39984.
(31) Lu, F.; Karlen, S. D.; Regner, M.; Kim, H.; Ralph, S. A.; Sun, R.-C.; Kuroda, K.-I.; Augustin, M. A.; Mawson, R.; Sabarez, H.; Singh, T.; Jimenez-Monteon, G.; Hill, S.; Harris, P. J.; Boerjan, W.; Mansfield, S. D.; Ralph, J. Naturally *p*-hydroxybenzoylated lignins in palms. *BioEnergy Res.* **2015**, *8* (3), 934−952.
(32) Kaal, J.; Serrano, O.; del Río, J. C.; Rencoret, J. Radically different lignin composition in *Posidonia* species may link to differences in organic carbon sequestration capacity. *Org. Geochem.* **2018**, *124*, 247−256.
(33) Rencoret, J.; Ralph, J.; Marques, G.; Gutiérrez, A.; Martínez, Á. T.; del Río, J. C. Structural characterization of the lignin from coconut (*Cocos nucifera*) coir fibers. *J. Agric. Food Chem.* **2013**, *61* (10), 2434−2445.
(34) Karlen, S. D.; Smith, R. A.; Kim, H.; Padmakshan, D.; Bartuce, A.; Mobley, J. K.; Free, H. C. A.; Smith, B. G.; Harris, P. J.; Ralph, J. Highly decorated lignins occur in leaf base cell walls of the Canary Island date palm *Phoenix canariensis*. *Plant Physiology* **2017**, *175* (3), 1058−1067.
(35) Zhang, Y.; Oates, L. G.; Serate, J.; Xie, D.; Pohlmann, E.; Bukhman, Y. V.; Karlen, S. D.; Young, M. K.; Higbee, A.; Eilert, D.; Sanford, G. R.; Piotrowski, J. S.; Cavalier, D.; Ralph, J.; Coon, J. J.; Sato, T. K.; Ong, R. G. Diverse lignocellulosic feedstocks can achieve high field-scale ethanol yields while providing flexibility for the biorefinery and landscape-level environmental benefits. *GCB Bioenergy* **2018**, *10* (11), 825−840.
(36) Fuchs, G.; Boll, M.; Heider, J. Microbial degradation of aromatic compounds - from one strategy to four. *Nat. Rev. Microbiol* **2011**, *9* (11), 803−816.
(37) Sibout, R.; Le Bris, P.; Legee, F.; Cezard, L.; Renault, H.; Lapierre, C. Structural redesigning Arabidopsis lignins into alkali-soluble lignins through the expression of *p*-coumaroyl-CoA:monolignol transferase PMT. *Plant Physiology* **2016**, *170* (3), 1358−1366.
(38) Kim, H.; Ralph, J.; Akiyama, T. Solution-state 2D NMR of ball-milled plant cell wall gels in DMSO-d_6. *BioEnergy Research* **2008**, *1* (1), 56−66.
(39) Mansfield, S. D.; Kim, H.; Lu, F.; Ralph, J. Whole plant cell wall characterization using solution-state 2D-NMR. *Nat. Protoc.* **2012**, *7* (9), 1579−1589.
(40) Kupče, E.; Freeman, R. Compensated adiabatic inversion pulses: Broadband INEPT and HSQC. *J. Magn. Reson.* **2007**, *187*, 258−265.
(41) Kim, H.; Padmakshan, D.; Li, Y.; Rencoret, J.; Hatfield, R. D.; Ralph, J. Characterization and elimination of undesirable protein residues in plant cell wall materials for enhancing lignin analysis by solution-state NMR. *Biomacromolecules* **2017**, *18* (12), 4184−4195.
(42) Kim, H.; Ralph, J. Solution-state 2D NMR of ball-milled plant cell wall gels in DMSO-d_6/pyridine-d_5. *Organic & Biomolecular Chemistry* **2010**, *8* (3), 576−591.
(43) Ralph, J.; Hatfield, R. D. Pyrolysis-GC-MS characterization of forage materials. *J. Agric. Food Chem.* **1991**, *39* (8), 1426−1437.
(44) Clifford, D. J.; Carson, D. M.; Mckinney, D. E.; Bortiatynski, J. M.; Hatcher, P. G. A new rapid technique for the characterization of lignin in vascular plants: Thermochemolysis with tetramethylammonium hydroxide (TMAH). *Org. Geochem.* **1995**, *23* (2), 169−175.
(45) Rencoret, J.; Kim, H.; Evaristo, A. B.; Gutiérrez, A.; Ralph, J.; del Río, J. C. Variability in lignin composition and structure in cell walls of different parts of macaúba (*Acrocomia aculeata*) palm fruit. *J. Agric. Food Chem.* **2018**, *66* (1), 138−153.
(46) Regner, M.; Bartuce, A.; Padmakshan, D.; Ralph, J.; Karlen, S. D. Reductive cleavage method for quantitation of monolignols and low-abundance monolignol conjugates. *ChemSusChem* **2018**, *11* (10), 1600−1605.
(47) Lu, F.; Ralph, J. Detection and determination of *p*-coumaroylated units in lignins. *J. Agric. Food Chem.* **1999**, *47* (5), 1988−1992.
(48) Bassett, I. J.; Crompton, C. W.; Woodland, D. W. The biology of Canadian weeds.: 21. *Urtica dioica L. Canadian Journal of Plant Science* **1977**, *57* (2), 491−498.
(49) Hartley, R. D.; Harris, P. J. Phenolic constituents of the cell walls of dicotyledons. *Biochemical Systematics and Ecology* **1981**, *9* (2−3), 189−203.
(50) Pollard, M.; Beisson, F.; Li, Y.; Ohlrogge, J. B. Building lipid barriers: biosynthesis of cutin and suberin. *Trends Plant Sci.* **2008**, *13* (5), 236−246.
(51) Bernards, M. A.; Lewis, N. G. The macromolecular aromatic domain in suberized tissue: a changing paradigm. *Phytochemistry* **1998**, *47* (6), 915−933.
(52) Waterhouse, A. L. Wine phenolics. *Ann. N.Y. Acad. Sci.* **2002**, *957*, 21−36.
(53) Vanholme, R.; Morreel, K.; Darrah, C.; Oyarce, P.; Grabber, J. H.; Ralph, J.; Boerjan, W. Metabolic engineering of novel lignin in biomass crops. *New Phytologist* **2012**, *196* (4), 978−1000.
(54) Xu, W. H.; Liang, Q.; Zhang, Y. J.; Zhao, P. Naturally occurring arbutin derivatives and their bioactivities. *Chem. Biodivers* **2015**, *12* (1), 54−81.
(55) Guleria, I.; Kumari, A.; Lacaille-Dubois, M.-A.; Nishant; Kumar, V.; Saini, A. K.; Dhatwalia, J.; Lal, S. Correction to: A review on the genus Populus: a potential source of biologically active compounds. *Phytochemistry Reviews* **2022**, *21* (4), 1047−1047.
(56) Potter, D.; Eriksson, T.; Evans, R. C.; Oh, S.; Smedmark, J. E. E.; Morgan, D. R.; Kerr, M.; Robertson, K. R.; Arsenault, M.; Dickinson, T. A.; Campbell, C. S. Phylogeny and classification of Rosaceae. *Plant Systematics and Evolution* **2007**, *266* (1−2), 5−43.
(57) Ralph, J.; Landucci, L. L., NMR of lignins. In *Lignin and Lignans; Advances in Chemistry*, Heitner, C.; Dimmel, D. R.; Schmidt, J. A., Eds.; CRC Press (Taylor & Francis Group): Boca Raton, FL, USA, 2010; pp 137−234.

https://doi.org/10.1021/acsomega.4c11429
ACS Omega 2025, 10, 6220−6227